Vaccine 37 (2019) 4382–4391

Contents lists available at ScienceDirect

Vaccine

journal homepage: www.elsevier.com/locate/vaccine

A DNA vaccine expressing an optimized secreted FAPα induces enhanced anti-tumor activity by altering the tumor microenvironment in a murine model of breast cancer

Fei Geng, Jie Guo, Qian-Qian Guo, Yu Xie, Ling Dong, Yi Zhou, Chen-Lu Liu, Bin Yu, Hui Wu, Jia-Xin Wu, Hai-Hong Zhang *, Wei Kong *, Xiang-Hui Yu *

National Engineering Laboratory for AIDS Vaccine, School of Life Science, Jilin University, Changchun 130012, PR China

ARTICLE INFO

Article history:
Received 11 November 2018
Received in revised form 29 May 2019
Accepted 7 June 2019
Available online 12 June 2019

Keywords:
FAPα
Cancer-associated fibroblast
Tumour microenvironment
Myeloid-derived suppressor cell
DNA vaccine
Cancer immunotherapy

ABSTRACT

Cancer-associated fibroblasts (CAFs), major components of the tumor microenvironment (TME), promote tumor growth and metastasis and inhibit the anti-tumor immune response. We previously constructed a DNA vaccine expressing human FAPα, which is highly expressed by CAFs, to target these cells in the TME, and observed limited anti-tumor effects in the 4T1 breast cancer model. When the treatment time was delayed until tumor nodes formed, the anti-tumor effect of the vaccine completely disappeared. In this study, to improve the safety and efficacy, we constructed a new FAPα-targeted vaccine containing only the extracellular domain of human FAPα with a tissue plasminogen activator signal sequence for enhanced antigen secretion and immunogenicity. The number of CAFs was more effectively reduced by $CD8^+$ T cells induced by the new vaccine. This resulted in decreases in CCL2 and CXCL12 expression, leading to a significant decrease in the ratio of myeloid-derived suppressor cells in the TME. Moreover, when mice were treated after the establishment of tumors, the vaccine could still delay tumor growth. To facilitate the future application of the vaccine in clinical trials, we further optimized the gene codons and reduced the homology between the vaccine and the original sequence, which may be convenient for evaluating the vaccine distribution in the human body. These results indicated that the new FAPα-targeted vaccine expressing an optimized secreted human FAPα induced enhanced anti-tumor activity by reducing the number of $FAP\alpha^+$ CAFs and enhancing the recruitment of effector T cells in the 4T1 tumor model mice.

1. Introduction

The tumor microenvironment (TME), which includes soluble factors, immune cells, endothelial cells, and cancer-associated fibroblasts (CAFs), plays important roles in tumorigenesis, invasion, and metastasis [1,2]. The TME not only provides nutrients for the growth of malignant tumor cells but also protects malignant tumor cells from the immune system by disrupting anti-tumor immune responses, while supporting those that are immunosuppressive [3,4]. It is noteworthy that the largest proportion of soluble factors related to tumor growth are secreted by stromal cells rather than malignant tumor cells themselves [5]. Therefore, targeting the TME for the treatment of malignant tumors has been extensively explored [3,6–8].

CAFs, as major components of tumor stromal cells surrounding the outer layer of tumor cells, promote tumor initiation, invasion, and metastasis via direct cellular interactions, stromal factors, or remodeling the extracellular matrix (ECM) [9–11]. These cells can recruit immunosuppressive cells, such as myeloid-derived suppressor cells (MDSCs), which have a remarkable ability to suppress T-cell responses [12], by secreting CCL2 and SDF-1 (CXCL12) into the TME [13–16]. ECM proteins, such as collagen I, secreted by CAFs are distributed around tumor cells to form a barrier that prevents chemotherapy drugs from entering the TEM and protects tumor cells from immune attack. Moreover, CAFs are genetically

Abbreviations: CAFs, Cancer-associated fibroblasts; TME, Tumor microenvironment; FAPα, Fibroblast activation protein α; SDF-1, Stromal cell-derived factor-1; Th1, T helper type 1; Th2, T helper type 2; Tregs, Regulatory T cells; MDSCs, Myeloid-derived suppressor cells; VEGFα, Vascular endothelial growth factor alpha; PDGF, Platelet-derived growth factor; qRT-PCR, Quantitative real time polymerase chain reaction; tPA, Tissue plasminogen activator.

* Corresponding authors at: No. 2699, Street Qianjin, School of Life Science, Jilin University, Changchun 130012, PR China.

E-mail address: Zhanghh@jlu.edu.cn (H.-H. Zhang).

https://doi.org/10.1016/j.vaccine.2019.06.012
0264-410X/

more stable than tumor cells, making them an attractive target for cancer immunotherapy [17,18].

Fibroblast activation protein α (FAPα), which is a type II membrane-bound serine protease with collagenase and dipeptidyl peptidase activities on CAFs, plays an important role in the remodeling of the tumor ECM [19,20]. As a major marker of CAFs, FAPα is expressed in over 90% of human epithelial carcinomas, such as breast cancer, colorectal cancer, lung cancer, and melanoma [21,22]. In normal tissues, FAPα expression is restricted to fibroblasts in embryonic tissues and wounds [21,23]. The deletion of FAPα$^+$ CAFs in the TME could significantly enhance the anti-tumor effect of cancer vaccines by eliminating immunosuppressive factors [24]. Importantly, human peripheral blood mononuclear cells can produce FAPα-specific cytotoxic T lymphocytes (CTL) under stimulation by FAPα [25].

In our previous work, a DNA vaccine expressing full-length human FAPα (CpVR-FAP) with the S624A mutation to block the dipeptidyl peptidase and gelatinolytic activities of FAPα was constructed; the vaccine had anti-tumor effects in both prophylactic and therapeutic settings in the 4T1 tumor model [26]. However, when the treatment time was delayed until the tumor was evident, the anti-tumor effect of the vaccine completely disappeared. Recent studies have supported claims that a mutant full-length FAPα (FAPα^{S624A}) still promotes tumor growth via non-enzymatic activities [27], and conserved amino acid sequences in the transmembrane region of FAPα play a crucial role in the dimerization and activity of FAPα [28]. Additionally, the tissue plasminogen activator (tPA) signal sequence has been proven to enhance the expression and secretion of antigens, thereby enhancing the immunogenicity of vaccines [29–31]. In this study, a new vaccine targeting FAPα, shF(m), was constructed containing only the extracellular domain of human FAPα (amino acids 27–760) with a mutation (S624A) and a tPA signal sequence fused to the N-terminal region for improved safety and efficacy. We also constructed a vaccine containing full-length mouse-derived FAPα, mF(m) (with the S624A mutation) to compare the anti-tumor effects of human and mouse-derived FAPα vaccines. The new FAPα-targeted vaccine, shF(m), induced stronger immunogenicity and anti-tumor activities than hF(m) (CpVR-FAP) and mF(m). All three vaccines could alter the tumor immunosuppressive microenvironment by decreasing the number of FAPα$^+$ CAFs and reducing the infiltration of MDSCs. Finally, we optimized the shF(m) sequence, minimized the nucleotide sequence homology with human FAPα, and constructed the sequence-optimized OshF(m) to facilitate clinical research and to improve expression in vivo. Taken together, our data suggest that the new FAPα-targeted vaccine expressing an optimized secreted FAPα leads to enhanced anti-tumor activity and strongly alters the tumor immunosuppressive environment; accordingly, it may be more suitable than previous FAPα-targeted vaccines for clinical applications.

2. Materials and methods

2.1. Construction of shF(m), mF(m), and OshF(m) plasmids

CpVR-hF(m) was the same plasmid as CpVR-FAP constructed previously [26]. The shF(m) fragment is a **s**hort form of human FAPα containing the extracellular domain (amino acids 27–760) and a tPA signal sequence at the N terminus. Fragment-mF(m) contained full-length mouse FAP, which was obtained from total RNA of mouse breast cancer tissues by RT-PCR using the following primer pair: 5′-GAAGATCTGCCGCCACCATGAAGACATGGCTGAAAAC3′ and 5′-CGGGATCCGTCGACTTAGTCTGATAAAGAAAAGCATTGC-3′. Fragment-OshF(m) had the same amino acid sequence as shF(m), but the nucleotide sequence homology was reduced to 76%. All fragments with a Kozak sequence at the N terminus and an amino acid mutation at 624 from S to A were cloned into the CpVR vector (VR1012 containing a CpG motif) to generate the plasmids CpVR-shF(m), CpVR-mF(m), and CpVR-OshF(m). The plasmids are referred to as hF(m), shF(m), mF(m), and OshF, respectively.

2.2. Mice and murine tumor model

Female BALB/c mice, aged 6–8 weeks, were purchased from Beijing Huafukang Biology Technology Co. Ltd. (Beijing, China) and kept in micro-isolator cages under pathogen-free conditions. All animal procedures were conducted according to the National Institutes of Health guide for the care and use of Laboratory animals (NIH Publications No. 8023, revised 1978). Murine 4T1 breast cancer cells were provided by the National Engineering Laboratory for AIDS Vaccine, Jilin University. To obtain a model of breast cancer in situ, BALB/c mice (eight per group) were challenged with 2×10^4 4T1 cells subcutaneously on the right lower flank. All mice were weighed every two days after tumor challenge. When the tumor mass was detectable, the tumor volume was measured every 2 days using calipers and calculated using the following formula: (length × width^2)/2 (mm^3). All experimental animals were euthanized within 30 days after tumor challenge for the tumor volume of mice in the Vec group was too large. For survival studies, the animals were monitored for approximately 45 days and animals were sacrificed when the humane endpoints were reached, including tumor ulceration, tumor size reaching 2000 mm^3, or decline in health (mice did not eat or had a severe weight loss).

2.3. Immunization of mice

For the immunogenicity assays, BALB/c mice (five per group) were immunized with plasmids (100 μg) three times into the skeletal muscle of both hind limbs every 2 weeks. In a prophylactic setting, BALB/c mice (eight per group) were immunized as the immunogenicity strategy, two weeks after the final immunization, the mice were challenged subcutaneously with 2×10^4 4T1 cells. There were two therapeutic settings, i.e., BALB/c mice (eight per group) were injected with 2×10^4 4T1 cells subcutaneously on day 0 and immunized with plasmids (100 μg) three times on days 2, 9, and 16 [Therapeutic setting (a)] *or* on days 7, 14, and 21 [Therapeutic setting (b)].

2.4. Cytotoxicity assay

The cytotoxicity assay was conducted in accordance with previously published procedures [32]. The three H-2Db-restricted FAPα peptides (LSPDRQFVY, VGPQEVPVP, and GGPCSQSVR) and unrelated peptides from human MUC1 (HGVTSAPDT, VTSAPDTRP, and APDTRPAPG) were incubated with target P815 cells for 2 h at 37 °C, and the target cells were labeled with different concentrations of CFSE fluorescent dye. Splenocytes from vaccinated mice were then incubated with the target cells for 6–8 h at 37 °C. Cytolytic activity was detected by flow cytometry and specific killing was calculated as follows: % killing = [1 − (peptide-loaded cells/unloaded cells from the immunized group)/(peptide-loaded cells/unloaded cells from the naïve group)] × 100. All of the peptides were synthesized by Shanghai GL Peptide Ltd. (Shanghai, China) at 95% purity.

2.5. IFN-γ ELISpot

The release of IFN-γ was detected using the BD^{TM} ELISPOT Kit (BD Biosciences, Franklin Lakes, NJ, USA). Briefly, 1×10^6 splenocytes were incubated with the peptides, as described for the cytotoxicity assay, and the procedure was performed according to

previously described methods [32]. IFN-γ secretion spots were counted and analyzed.

2.6. Cytokine IL-2 detection by ELISA

Splenocytes (1×10^7) from vaccinated mice were stimulated with FAPα (99–499 aa) at a concentration of 5 μg/mL for 5 days in a 12-well plate. The cell culture supernatants were then collected to detect the expression of secreted IL-2 using the Mouse IL-2 ELISA MAX™ Standard Set (BioLegend, San Diego, CA, USA) according to the manufacturer's instructions. The culture medium was diluted 1:3 in PBS with 1% FBS for detection.

2.7. Quantitative real-time PCR (qRT-PCR)

The procedure for qRT-PCR was published previously [33]. qRT-PCR primers for *IL-2, IL-4, IL-6, IL-10, IFN-γ, TNF-α, TGF-β, GzmB, GM-CSF, PD-L1, FoxP3, FAPα, collagen I, SDF-1 (CXCL12), CCL2, VEGFα* and *PDGF*were used to detect mRNA expression levels in splenocytes or tumor tissues. *GAPDH* was used as an internal reference.

2.8. Determination of $CD3^+$, $CD4^+$, $CD8^+$ T cells, $FAP\alpha^+$ CAFs, Tregs and MDSCs

Tumors were minced and dissociated using Liberase (Roche, Basel, Switzerland) at 0.04 mg/mL for 2 h and then passed through a 0.45-mm nylon mesh to obtain the single cell suspension.

For the detection of $CD4^+$ and $CD8^+$ T cells, separated splenic or tumor cells were washed with PBS and stained with anti-mouse CD45 PE, anti-mouse CD3 FITC, anti-mouse CD4 PE-CY7, and anti-CD8 APC (all from BioLegend) for 25 min at 4 °C. Thereafter, the samples were washed twice with staining buffer and analyzed by flow cytometry. For the detection of $FAP\alpha^+$ CAFs, separated tumor cells were washed with PBS and immunostained with a rabbit anti-FAPα antibody (Abcam, Cambridge, UK) or normal rabbit IgG control antibody at 4 °C for 60 min. After washing, cells were stained with sheep anti-rabbit FITC secondary antibody (BioLegend) for 25 min. Flow cytometry was performed for detection after washing two times. For the detection of Tregs, the eBioscience™ Mouse Regulatory T Cell Staining Kit #1 was used, and the procedure was performed according to the manufacturer's instructions. For the detection of MDSCs, the Mouse MDSC Flow Cocktail 1 (BioLegend) was used, Separated tumor cells were washed with PBS and immunostained with an anti-mouse CD11b-PE, anti-mouse Gr-1 APC, and anti-mouse Ly-6G FITC for 25 min at 4 °C. After two washes, all samples were analyzed by flow cytometry.

2.9. Statistical analysis

All in vivo and in vitro experiments were performed at least three times. Data were analyzed using one-way ANOVA. Differences between groups were assessed for statistical significance using the unpaired *t*-test. $P < 0.05$ was considered significant and $P < 0.01$ was considered highly significant. All statistical analyses were implemented in GraphPad Prism 7.0.

3. Results

3.1. Construction, identification, and expression of DNA vaccines

Mutant full-length FAPα ($FAP\alpha^{S624A}$) still promotes tumor growth via non-enzymatic activity [27] and the conserved amino acid sequence in the transmembrane region of FAPα plays a crucial role in the dimerization and activity of FAPα [28]. Accordingly, we optimized the previously developed FAPα vaccine [CpVR-FAP, referred to as hF(m) in this paper] [26]. The new FAPα vaccine, shF(m), contained only the extracellular domain of human FAPα (amino acids 27–760) and a tPA signal sequence fused to the N-terminal region to enhance protein extracellular secretion and immunogenicity [29–31]. To compare the anti-tumor effects of human and mouse FAPα vaccines on mouse mammary gland models, a full-length mouse FAPα vaccine, mF(m), containing the S624A mutation was constructed. The structures of the three vaccines are shown in Fig. 1A. After constructing the eukaryotic expression vectors shF(m) and mF(m) as described in the Materials and Methods, FAPα fragments were verified by restriction enzyme digestion (Fig. 1B) and western blotting with an antibody against FAPα (using GAPDH as control) (Fig. 1C).

3.2. shF(m) has strong immunogenicity

To evaluate the immunogenicities of the three vaccines, four groups of BALB/c mice (n = 5) were immunized according to the schedule shown in Fig. 2A. The Vec, hF(m), shF(m), and mF(m) groups were immunized with the CpVR vector, hF(m), shF(m), and mF(m), respectively. Two weeks after the final immunization, all mice were sacrificed, and isolated splenocytes were used to detect cellular immune responses by ELISpot and CTL assays. The shF(m) group exhibited higher frequencies of FAPα-specific IFN-γ-secreting $CD8^+$ T cells, as detected by ELISpot ($P < 0.01$) and more effective CTL responses at an E:T ratio of 100:1 ($P < 0.05$) than those of other groups (Fig. 2B and C). After sacrifice, splenocytes were prepared and stimulated by FAPα peptides for 2 days, and the proportions of $CD3^+$, $CD3^+CD8^+$, and $CD3^+CD4^+$ T cells were analyzed by FACS (Fig. 2D). The proportions of $CD3^+$ T cells in splenocytes of the hF(m) group, shF(m) group, and mF(m) group were significantly higher than that of the Vec group, and the shF(m) group vaccinated shF(m) showed better results in terms of both $CD3^+CD8^+$ and $CD3^+CD4^+$ T cells compared with hF(m) group, indicating improved immune responses ($P < 0.05$). Compared with mF(m), shF(m) had no significant improvement in the ability to

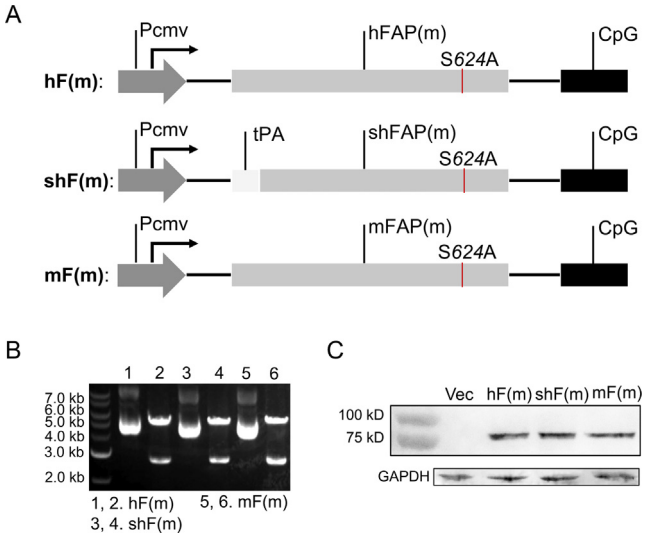

Fig. 1. Construction of DNA vaccines shF(m) and mF(m) and identification of protein expression. (A) Schematic representation of the three DNA plasmids, as verified by nucleotide sequencing. (B) Agarose gel electrophoresis of plasmids and restriction enzyme digestion products for the identification of FAPα fragments in the three plasmids. (C) Protein expression of FAPα was verified by western blotting after the transient transfection of 293T cells. All data are representative of one out of three experiments, with similar results.

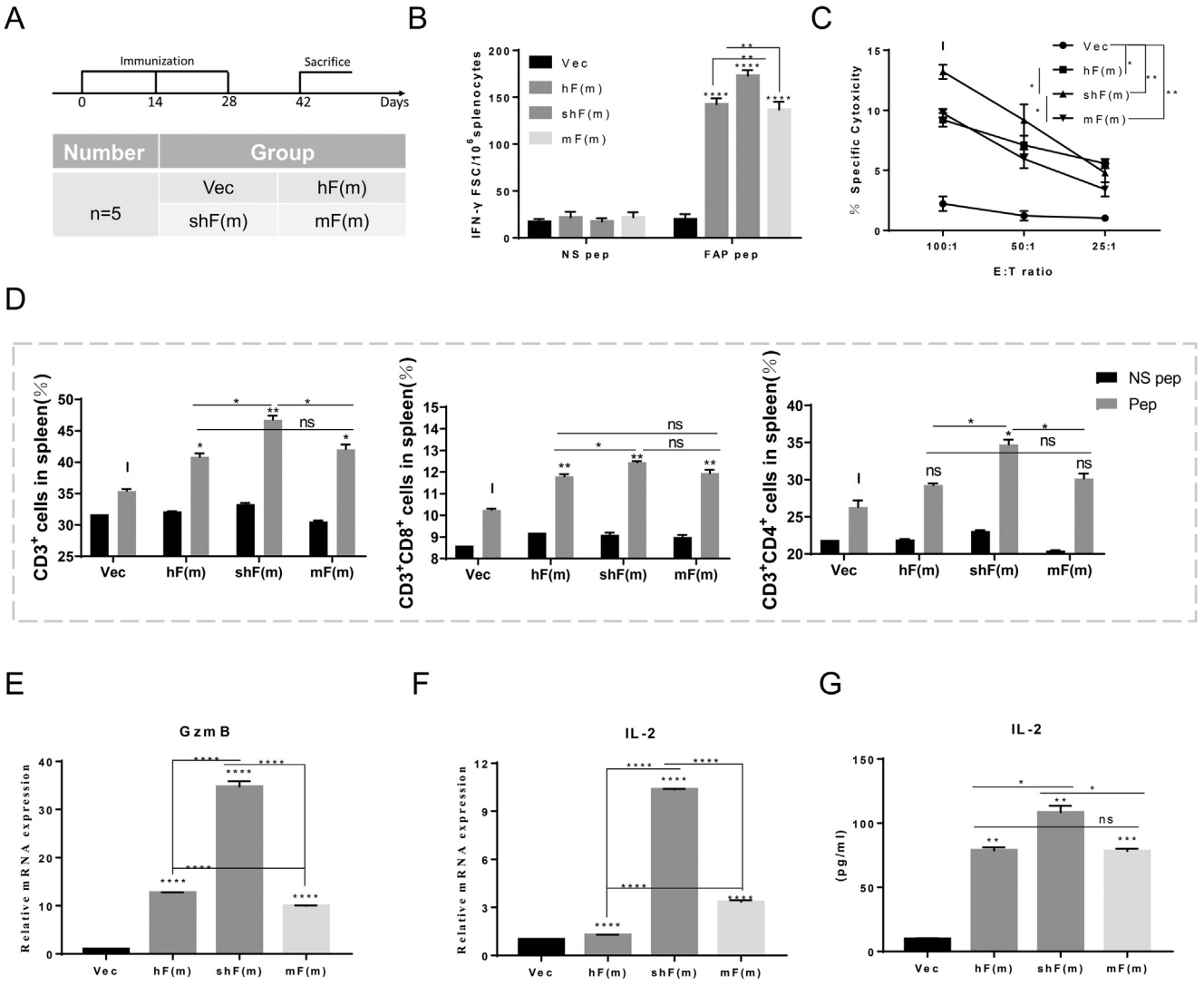

Fig. 2. Analysis of the immunogenicity of different vaccines. (A) Immunization regimens. BALB/c mice (n = 5) were immunized three times intramuscularly on day 0, 14, and 28 and sacrificed on day 42. (B) Splenocytes from different mouse groups were stimulated with FAPα peptides and unrelated human MUC1 peptides (negative control) for ELISpot assays (SFC, spot-forming cells). (C) For the in vitro CTL assay, splenocytes of different mouse groups were incubated with P815 cells as target cells, which were incubated with a mixture of FAPα peptides or unrelated human MUC1 peptides (data not shown) at E:T ratios of 25:1, 50:1, and 100:1 ($^{*}P < 0.05$; $^{**}P < 0.01$). (D) Frequencies of $CD3^+$, $CD3^+CD4^+$, and $CD3^+CD8^+$ T cells in 5×10^4 splenocytes in the five mouse groups were detected by FCM after incubation with FAPα peptides or unrelated human MUC1 peptides as a control for 48 h ($^{*}P < 0.05$; $^{**}P < 0.01$). (E), (F) Relative mRNA expression levels of *GzmB* and *IL-2* in splenocytes were confirmed by qRT-PCR ($^{*}P < 0.05$; $^{**}P < 0.01$; $^{***}P < 0.001$; $^{****}P < 0.0001$). (G) Secretion of IL-10 from splenocytes was detected using the ELISA MAXTM Set ($^{*}P < 0.05$; $^{**}P < 0.01$; $^{***}P < 0.001$).

induce CD3 + CD8+ T cells, but it had a stronger ability to induce CD3 + CD4+ T cells ($P < 0.05$). The relative expression levels of *GzmB* and *IL-2* in unstimulated splenocytes of the shF(m) group were 5-fold and 3-fold higher than those in splenocytes of the hF (m) group (Fig. 2E and F, $P < 0.0001$). In the culture medium secreted by splenocytes stimulated by FAPα, IL-2 expression was higher in the shF(m) group than that in the other groups (Fig. 2G, $P < 0.05$). The difference in the expression of IL-2 at protein and mRNA levels did not exactly match, possibly because the protein level exhibited the ability of splenocytes to secrete IL-2 after antigen stimulation, while mRNA level exhibited levels of IL-2 mRNA of splenocytes without antigen stimulation. And the protein expression and the mRNA expression levels of the gene were not exactly matched at times. However, both experimental results demonstrated that shF(m) could significantly enhance the expression of IL-2 in splenocytes of immunized mice. These results indicated that the new FAPα-targeting vaccine, shF(m), induced stronger immunogenicity than hF(m) and mF(m). We also found that the human FAPα vaccine [hF(m)] and mouse FAPα vaccine [mF(m)] induced similar immune responses, as shown in Fig. 2B–G.

3.3. In a prophylactic setting and different therapeutic settings, shF(m) shows remarkable improvements in 4T1 growth inhibition

First, we evaluated the preventive effect of the vaccines. BALB/c mice (n = 8) were immunized and inoculated with tumor cells according to the strategy shown in Fig. S1A. Tumor growth was monitored for 23 days after inoculation. As shown in Fig. S1B, all vaccines could inhibit the growth of tumors, but shF(m) was more effective than other vaccines in terms of size and weight of tumors ($P < 0.001$). To further explore the anti-tumor effect of different FAPα-targeting vaccines, we examined the therapeutic effectiveness of vaccines. BALB/c mice (n = 8) were inoculated subcutaneously with 2×10^4 4T1 cells into the right lower flank and treated with different vaccines and the CpVR vector as a control [Therapeutic setting (a) described in the Materials and Methods]

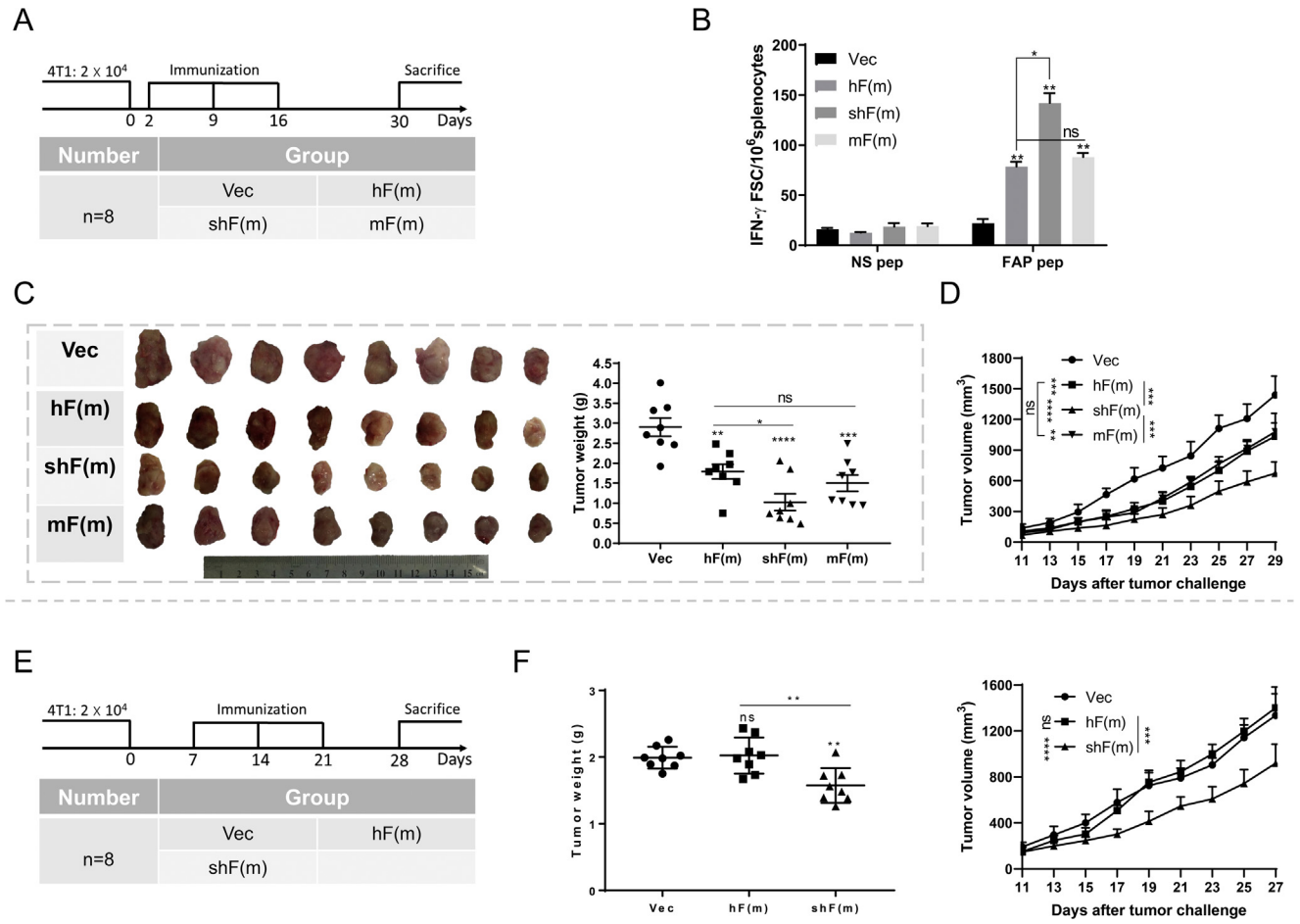

Fig. 3. Enhancement of immune responses and anti-tumor effects of shF(m) for different treatment strategies. (A) In Therapeutic setting (a), BALB/c mice (n = 8) were inoculated with 2×10^4 4T1 tumor cells on day 0 and treated after 2 days. (B) ELISPOT analysis of different mouse groups using FAPα peptides to stimulate splenocytes, with unrelated human MUC1 peptides as a control ($^{*}P < 0.05$; $^{**}P < 0.01$). (C) Images of tumor nodes (left) and tumor weight measured after killing (right) in each of the four groups ($^{*}P < 0.05$; $^{**}P < 0.01$; $^{***}P < 0.001$; $^{****}P < 0.0001$). (D) Tumor growth was measured every 2 days for 29 days after the tumor challenge. ($^{***}P < 0.001$; $^{****}P < 0.0001$) (E) In Therapeutic setting (b), BALB/c mice (n = 8) were inoculated with 2×10^4 4T1 tumor cells on day 0 and treated after 7 days. (F) Tumor weights (left) and tumor growth curves (right) of (E) are shown as means ± SD ($^{**}P < 0.01$).

(Fig. 3A). The number of FAPα-specific IFN-γ-secreting $CD8^+$ T cells in splenocytes of the shF(m) group was significantly higher than that of hF(m) group based on ELISpot results (Fig. 3B, $P < 0.05$). Tumor weights and tumor growth kinetics (Fig. 3C and D) were measured and tumor images were obtained after killing. When mice were vaccinated with shF(m), tumor growth was markedly inhibited compared with hF(m) group (Fig. 3C (right) and 3D, $P < 0.05$). In Fig. 3C (left), a macroscopic image of the tumor nodes in the four groups (n = 8) is displayed.

To further verify the effectiveness of the shF(m) vaccine, we delayed the treatment to days 7 after BALB/c mice (n = 8) were inoculated subcutaneously with 4T1 cells, when subcutaneous tumor nodes were detectable. The treatment strategy [Therapeutic setting (b) described in the Materials and Methods] is shown in Fig. 3E. In this therapeutic setting, shF(m) still had a strong anti-tumor effect, but hF(m) had almost no tumor suppressive effect (Fig. 3F, $P < 0.01$).

These results proved that shF(m) significantly inhibited the growth of 4T1 tumors, irrespective of whether it was applied before or after tumor formation in mice. In addition, the inhibitory effects of mF(m) and hF(m) on 4T1 tumor growth were the same (Fig. 3C), proving that the mouse FAPα vaccine could break the immune tolerance and induce an anti-tumor immune response against mouse FAPα [34–36]. Therefore, a human FAPα vaccine, such as shF(m), may have similar therapeutic effects on human solid tumors.

3.4. shF(m) promotes the infiltration of $CD8^+$ T cells, induces immune-enhancing factors, and reduces immunosuppressive factors in the TME

To determine why hF(m) lost its inhibitory effect on tumor growth when it was applied after tumor node formation (Fig. 3D), the percentages of infiltrated $CD3^+CD8^+$ and $CD3^+CD4^+$ T lymphocytes in $CD45^+$ cells were verified by flow cytometry. The percentage of infiltrated $CD3^+CD8^+$ T lymphocytes in the shF(m) group was nearly 2-fold higher than that in the hF(m) group; these cells are crucial for tumor immunotherapy (Fig. 4A right, $P < 0.05$). At the same time, we found that both vaccines reduced the proportion of infiltrated $CD4^+CD25^+Foxp3^+$ Tregs in $CD4^+$ cells, and shF(m) was more capable of reducing Tregs (Fig. 4B, $P < 0.01$). A qRT-PCR analysis showed that the expression levels of various Th1 cytokines (*IL-2*, *TNF-α*, and *IFN-γ*) and *GzmB* in the shF(m) group were significantly higher than those in the hF(m) group (Fig. 4C, $P < 0.001$). Additionally, the expression levels, of various Th2 cytokines (*IL-4*, *IL-6*, and *TGF-β*) and *GM-CSF* in the shF(m) group showed remarkable reductions (Fig. 4D, $P < 0.05$). Similar to our previous results, there was a slight increase in the level of *IL-10* expression in the hF(m) group compared to the control group, but this phenomenon was not found in the shF(m) group (Fig. 4D). The reason for this may be that the both vaccines reduced the proportion of Tregs in $CD4^+$ T cells, but simultaneously promoted

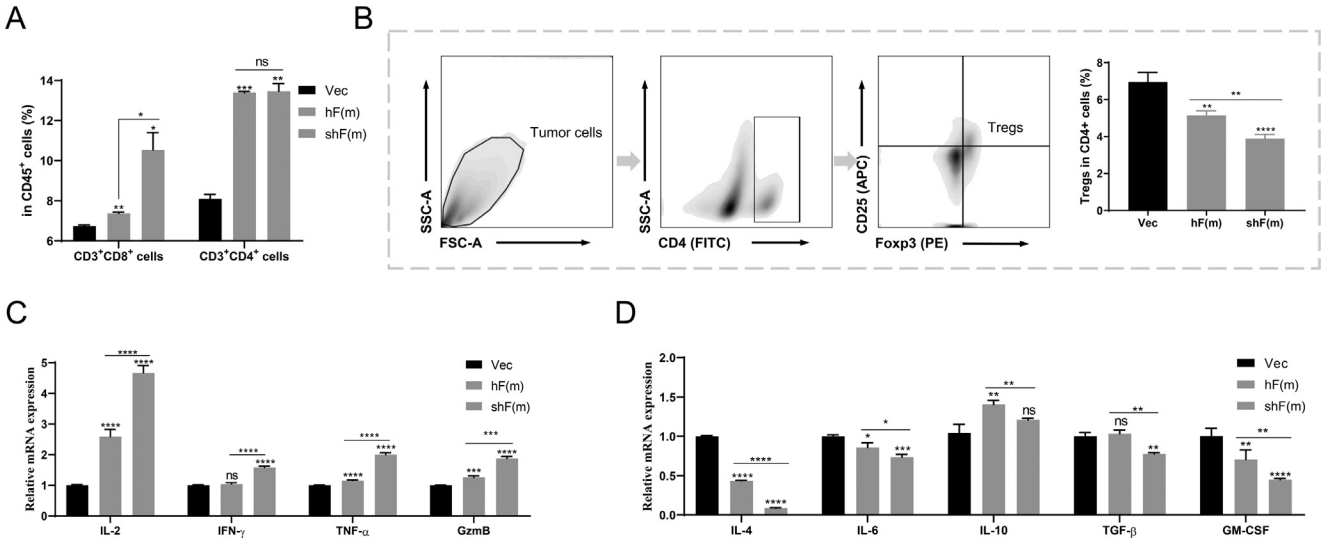

Fig. 4. Detection of CD8$^+$ and CD4$^+$ T cells, Tregs and the expression of inflammatory factors in tumors. (A) Percentages of infiltrated CD3$^+$CD8$^+$ and CD3$^+$CD4$^+$ T lymphocytes in CD45$^+$ cells of tumors were verified by flow cytometry ($^*P < 0.05$; $^{**}P < 0.01$; $^{***}P < 0.001$). (B) The proportion of infiltrated CD4$^+$CD25$^+$Foxp3$^+$ Tregs in CD4$^+$ T cells. The gating strategy is shown on the left ($^{**}P < 0.01$; $^{****}P < 0.001$). (C) Relative mRNA expression levels of various Th1 cytokines (*IL-2, TNF-α,* and *IFN-γ*) and *GzmB* were detected by qRT-PCR ($^{***}P < 0.001$; $^{****}P < 0.0001$). (B) Relative mRNA expression levels of various Th2 cytokines (*IL-4, IL-6, IL-10* and *TGF-β*) and *GM-CSF* were detected by qRT-PCR ($^*P < 0.05$; $^{**}P < 0.01$; $^{***}P < 0.001$); $^{****}P < 0.001$).

the infiltration of CD4$^+$ T cells (Fig. 4A), while shF(m) had a stronger ability to reduce Tregs, so there was no increase of *IL-10* expression compared with hF(m) (Fig. 4D, $P < 0.01$). These results demonstrated that shF(m) could induce more powerful anti-4T1 tumor immune responses by inducing a shift in local immunity from Th2 to Th1, although *IL-10* levels in tumors were slightly up-regulated (data not displayed). In addition, the safety of full-length FAPα may explain the failure of hF(m) in this tumor model [27,28].

3.5. shF(m) reduces CCL2 and SDF-1 levels by targeting FAPα, thereby decreasing MDSC infiltration in the tumor microenvironment

MDSCs, a diverse population of immature myeloid cells, are present in a wide range of tumor types; they promote tumorigenesis and progression and are a barrier to many tumor treatments [37]. Previous studies have revealed that FAPα$^+$ CAFs in the TME inhibit the anti-tumor immune response by recruiting large quantities of MDSCs via CCL2 and SDF-1 (CXCL12) [14–16]. To determine whether our FAP-targeted vaccines reduce MDSC infiltration in tumors by eliminating CAFs in the TME, we performed flow cytometry to identify MDSCs and FAPα$^+$ CAFs in primary tumors. As shown in Fig. 5A and B(left), the three different FAP-targeted vaccines reduced both FAPα$^+$ CAFs and MDSCs in the TME, and vaccination with shF(m) markedly reduced the percentages of FAPα$^+$CAFs and MDSCs compared with vaccination with hF(m) ($P < 0.05$). The gene expression levels of *FAPα* and *collagen I* decreased with the clearance of FAPα$^+$ CAFs (Fig. 5B left and Fig. 5C, $P < 0.001$). The expression levels of *CCL2* and *SDF-1* decreased significantly, which led to a reduction in the number of infiltrated MDSCs in the TME (Fig. 5D, $P < 0.0001$). Due to the decrease in the proportion of CAFs, factors in the TME that benefit tumor progression, such as *VEGFα* and *PDGF*, were also reduced (Fig. 5E, $P < 0.0001$). Based on these results, FAP-targeted vaccines could decrease the number of FAPα$^+$ CAFs and reduce the expression levels of CCL2 and SDF-1, thereby reducing MDSC infiltration in the tumor. shF(m) showed a better regulatory effect in the TME than those of hF(m) and mF(m), which had similar effects.

3.6. OshF(m) and shF(m) have similar anti-tumor activity, but OshF(m) has a stronger ability to alter the tumor microenvironment

To facilitate future clinical research and improve vaccine expression in vivo, we optimized the nucleotide sequence of shF(m) and reduced the sequence homology for the monitoring of the vaccine distribution in vivo (Fig. 6A). The newly optimized shF(m) was called OshF(m). The expression of FAPα in the OshF(m) group was significantly higher than that of shF(m), as verified by western blotting (Fig. 6B). The results of prophylactic experiment showed that OshF(m) had better effect than shF(m) in inhibiting the growth of tumors (Fig. S1C, $P < 0.05$). To compare OshF(m) and shF(m) with respect to the anti-tumor effect and regulatory ability in the TME, in a therapeutic setting, we set up three groups of mice (n = 8), i.e., a Vec group, OshF(m) group, and shF (m) group. Mice were immunized once a week on the seventh day after tumor challenge (2×10^4 4T1 cells) and were immunized three times (Fig. 6C). Unlike the results of prophylactic experiment, there was no significant difference between OshF(m) and shF(m) in the inhibition of tumor growth and induction of the anti-tumor immune response (Fig. 6D, F, and G). The same three groups of mice (n = 12) were vaccinated according to the therapeutic settings to evaluate survival time. OshF(m) and shF(m) prolonged the survival of mice to a certain extent compared with that of the control group, but there was still no significant difference between the two groups. However, the relative expression levels of *FAPα*, *SDF-1*, and *collagen I*, which are indicators of the level of CAFs, in the OshF(m) group were significantly lower than those in the shF(m) group (Fig. 6H, I, and J, $P < 0.05$). Flow cytometry showed that the infiltrated MDSCs in the OshF(m) and shF(m) groups were dramatically reduced (Fig. 6K, $P < 0.01$). In addition, the application of the vaccines did not affect the weight growth of mice (Fig. S2). Thus, OshF(m) and shF(m) had similar effects on tumor suppression and survival in mice in a therapeutic setting, but OshF(m) had stronger ability to inhibit tumor growth in a prophylactic setting.

4. Discussion

Recent advances in cancer immunotherapy, such as the development of immune checkpoint inhibitors and chimeric antigen

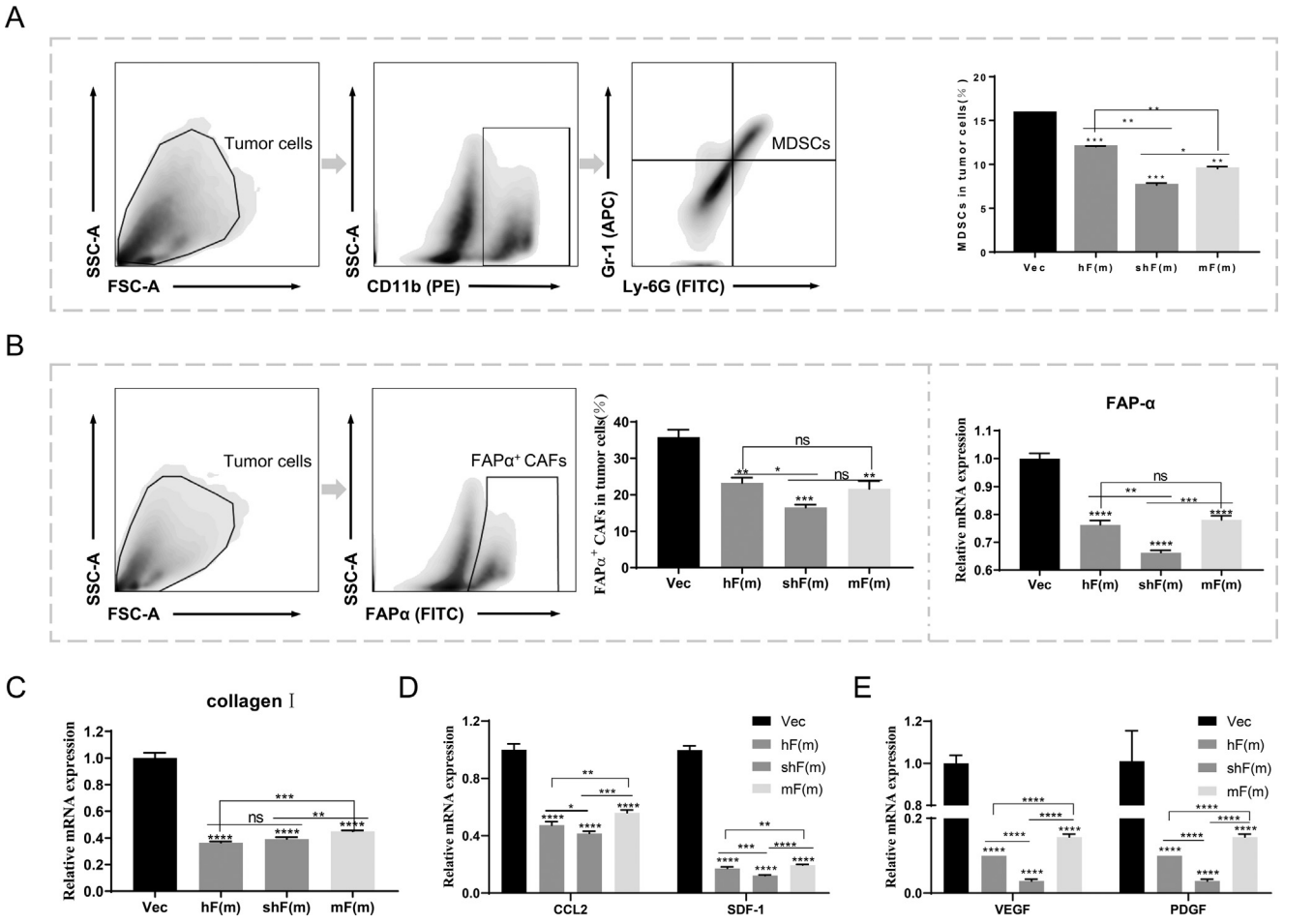

Fig. 5. Comparison of the regulatory effects of the three vaccines on the tumor microenvironment. (A) The proportion of MDSCs in the tumor was detected by flow cytometry. The gating strategy is shown using representative dot plots of MDSCs ($^{*}P < 0.05$; $^{**}P < 0.01$; $^{***}P < 0.001$). (B) The proportion of FAPα^{+}CAFs (left) and was detected by flow cytometry and the relative mRNA expression levels of *FAPα* (right) in tumors were detected by qRT-PCR ($^{*}P < 0.05$; $^{***}P < 0.01$; $^{***}P < 0.001$; $^{****}P < 0.0001$). (C) Relative mRNA expression levels of collagen I in tumors were detected by qRT-PCR ($^{****}P < 0.0001$). (D) Relative mRNA expression levels of *CCL2* and *SDF-1* (*CXCL12*) in tumors were detected by qRT-PCR ($^{*}P < 0.05$; $^{***}P < 0.01$; $^{***}P < 0.001$; $^{****}P < 0.0001$). (E) Relative mRNA expression levels of *VEGF* and *PDGF* in tumors were detected by qRT-PCR ($^{****}P < 0.0001$).

receptor T cell therapies, have pushed cancer therapy into a new era [38–41]. However, a relatively small fraction of patients benefit from these approaches due to an immunosuppressed tumor microenvironment, which provides nutrients for tumor growth and suppresses the immune system [1–3,7]. As a major part of the TME, CAFs have a prominent role in the growth, progression, and metastasis of tumors by producing soluble factors that modulate the ECM [9–11]. In addition, their genetic stability makes CAFs an attractive target for cancer immunotherapy [17,18].

Several studies, including our previous work, have verified that cancer vaccines targeting FAPα, which is expressed on CAFs, attenuate tumor growth by inducing CD8^{+} T cell infiltration, which ultimately reduce the number of CAFs and eliminates immunosuppressive components in the TME [10,26,32,35,36,42]. In addition, more than 90% of epitheliomas, such as breast cancer, colorectal cancer, pancreatic cancer, and lung cancer, express FAPα [21,22], and high expression levels of FAPα in tumor stroma are associated with aggressive progression, metastasis, and recurrence in many different cancer types [43–45], suggesting that FAPα is a promising treatment target for various cancers. In the studies of immunotherapies targeting FAPα, the anti-tumor effects induced by cancer vaccines were detected in prophylactic settings or therapeutic settings, in which vaccines were administered to mice only a few days after tumor inoculation [10,26,32,35,36,42]. To verify the efficacy of therapies targeting FAPα, it is necessary to delay the treatment time until after tumor establishment in mice to mimic real clinical cases (Fig. 4D). In this model, the anti-tumor effect of CpVR-FAP, a DNA vaccine targeting FAPα constructed in our previous work [26], almost completely disappeared (Fig. 4E). Recent studies have shown that full-length FAPα with the S624A mutation still promotes tumor growth via non-enzymatic activity [27], and a specific transmembrane region plays a crucial role in the dimerization and activity of FAPα [28]. These previous studies indicate that vaccines containing full-length FAPα have safety issues. Furthermore, the immunogenicity of vaccines needs to be improved. tPA signal sequences have the capacity to elicit cell-mediated and humoral immune responses in vaccinated animals and are used extensively in the construction of viral and DNA vector vaccines. To enhance the safety and efficacy of the vaccine, we constructed a new FAPα-targeted vaccine [shF(m)] that only contains the extracellular domain of human FAPα (amino acids 27–760) and a tPA signal sequence fused to the N-terminal region.

shF(m) induced more FAPα-specific CTLs than hF(m) (CpVR-FAP), which are crucial for the therapeutic efficacy of tumor vaccines. The isolated splenocytes from the shF(m) group could secrete more IL-2 in vitro and the relative expression levels of IL-2 and GzmB were up-regulated. Furthermore, the vaccine overcame the immunosuppressive environment, facilitated an increase

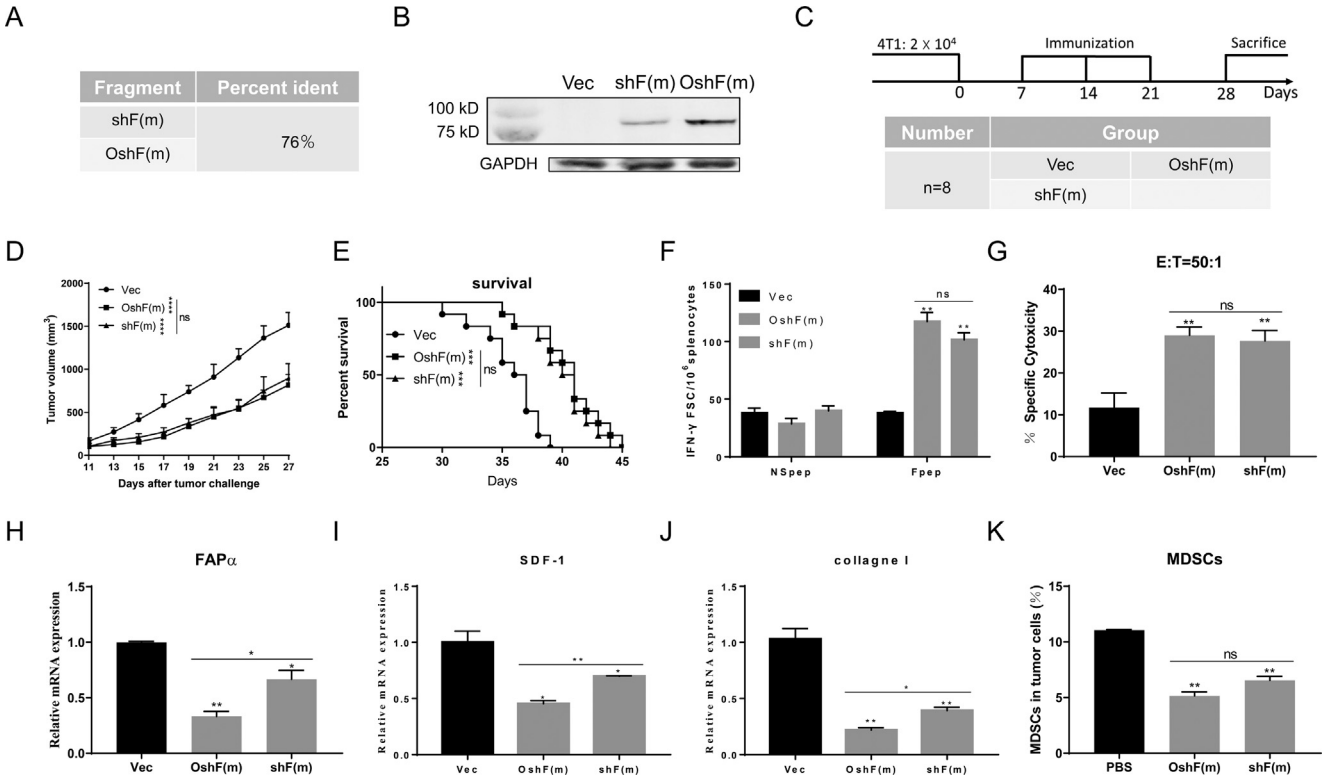

Fig. 6. Construction of OshF(m) and comparison of anti-tumor activity and regulation of the tumor microenvironment between OshF(m) and shF(m). (A) DNA sequence homology between shF(m) and OshF(m). (B) Protein expression of FAPα was verified by western blotting after the transient transfection of 293T cells. (C) BALB/c mice (n = 8) were inoculated with 2×10^4 4T1 tumor cells on day 0 and treated after 7 days. (D) Tumor growth was monitored and measured every 2 days for 27 days after the tumor challenge. Tumor growth in each of the four groups (n = 8) is depicted as the mean ± SD ($^{****}P < 0.0001$). (E) Survival time (n = 12) was monitored for 45 days, and the mean survival times were as follows: Vec group = 36.5 days, OshF(m) group = 41 days, shF(m) group = 40.5 days ($^{***}P < 0.001$). (F) ELISPOT assays were conducted using splenocytes from three mouse groups stimulated with FAPα peptides or unrelated human MUC1 peptides (nonspecific peptides) ($^{**}P < 0.01$) (G) CTL assays were conducted using target cells (E:T ratio = 50:1) ($^{**}P < 0.01$). (H), (I), (J) Relative mRNA expression levels of *FAPα, SDF-1,* and *collagen I* in tumors were detected by qRT-PCR ($^{*}P < 0.05$; $^{**}P < 0.01$). (K) Ratios of infiltrated MDSCs in tumors of the three mouse groups were detected and analyzed by flow cytometry on day 27 after tumor inoculation ($^{**}P < 0.01$).

in $CD8^+$ T cell infiltration in an established 4T1 tumor model, and induced a shift in local immunity from Th2 to Th1, which is more conducive to tumor destruction [10]. To compare the anti-tumor effects of human and mouse FAPα vaccines on mouse mammary gland models, a DNA vaccine expressing full-length mouse FAPα, mF(m), was constructed (Fig. 1A). The results (Figs. 1 and 3B, C) showed that hF(m) and mF(m) had similar intensities with respect to immunogenicity and the inhibition of tumor growth. Furthermore, human FAPα could stimulate human peripheral blood mononuclear cells to produce FAPα-specific T cells, which proves that a human FAPα vaccine could be used for human cancer immunotherapy [25]. Among the vaccines examined, shF(m) had the strongest anti-tumor activity and was most suitable for the clinical treatment of human cancers.

Tumors escape from surveillance and elimination by the immune system by a variety of complementary immunosuppressive mechanisms, such as the downregulation of MHCI, upregulation of surface immunosuppressive ligands (e.g., PDL-1), increases in the expression of immunosuppressive factors (e.g., IL-10, TGF-β), and recruitment of various immunosuppressive cells (e.g., Tregs, MDSCs) into the TME [1–4]. CAFs could promote the recruitment and function of MDSCs via the secretion of CCL2 and SDF-1 (CXCL12) and inhibit the function of effector T cells via the secretion of TGF-β [14–16,46]. The FAPα-targeted vaccine shF(m) effectively decreased the number of $FAP\alpha^+$ CAFs in the TME, reducing the expression of CCL2 and CXCL12, thereby decreasing the infiltration of MDSCs. The expression levels of factors related to immunosuppression in the TME were also weakened. Accordingly, targeting $FAP\alpha^+$ CAFs may relieve immunosuppression and ECM barrier function in the TME [9,10,17].

Furthermore, we developed a codon-optimized shF(m) fragment, OshF(m), with similar inhibitory effects on tumor growth and improvements in mouse survival to those of shF(m), but more effective removal CAFs and immunosuppressive molecules in the TME, which may improve the outcomes of immunotherapy and chemotherapy [32,34,35,42]. Moreover, the nucleotide sequence of the OshF(m) fragment had only 76% homology with the original sequence, which is convenient for detecting the distribution of the vaccine in the human body in future clinical applications.

Interestingly, despite the OshF(m) vaccine enhancing anti-tumor T cell immune responses and reducing the number of CAFs in the TME, this did not significantly prolong the survival time of mice. This may be due to that all vaccines mentioned in this article targeted only at one single antigen (FAPα), which made the immune responses induced by the vaccines only act on $FAP\alpha^+$ CAFs. Even though OshF(m) could regulate the TME, there is still a lack of treatment for cancer cells. Previous studies have shown that a cancer cell vaccine expressing FAPα can target both cancer cells and $FAP\alpha^+$ CAFs, and significantly prolong the survival time of mice compared with single cancer cell vaccine [42]. Therefore, OshF(m) might have a better therapeutic effects if it was combined with other vaccines targeting cancer cells.

Single therapy that can effectively cure malignancies are generally lacking, especially for metastatic and recurrent tumors. Vaccines targeting FAPα may not only reduce CAFs by inducing massive effector CTLs but may also allow CTLs to destroy the matrix barrier

of the TME to enter the tumor. Other studies and our current work have reported excellent anti-tumor effects when FAPα-targeted immunotherapy is combined with chemotherapy or other tumor-targeted vaccines [32,34,35,42]. Therefore, immunotherapies targeting FAPα need to be combined with other therapies, such as chemotherapy, surgery, radiotherapy, and other immunotherapies, to achieve a better therapeutic effect.

In summary, our findings demonstrate the efficacy of a DNA vaccine expressing an optimized secreted FAPα in inducing FAPα-specific $CD8^+$ T cells to target CAFs and destroy the TME. This vaccine is suitable for future clinical research owing to its low homology with the original sequence. Moreover, the tumor model in this study was a wild-type tumor-bearing mouse model, in which the level of antigen expression is close to real pathological conditions, which could better reflect the authenticity and effectiveness of the vaccine compared with tumor models expressing exogenous proteins. These results provide a basis for the clinical treatment of breast cancer using an FAPα-targeted vaccine.

Acknowledgements

Funding: We are grateful for the support of the Specialized Research Fund for the National Natural Science Foundation of China (No. 31300765), the National Science, Technology Major Project of the Ministry of Science and Technology of China (No. 2018ZX09301050-003 and 2014ZX09304314-001), Jilin Province Science and Technology Program (No. 20180201001YY and 20160519018JH), and Changchun City Science and Technology Plan Project (No. 17YJ002).

Declaration of Competing Interest

The authors declare that they have no conflict of interest.

Appendix A. Supplementary data

Supplementary data to this article can be found online at https://doi.org/10.1016/j.vaccine.2019.06.012.

References

[1] Hu M, Polyak K. Microenvironmental regulation of cancer development. Curr Opin Genet Dev 2008 Feb;18(1):27–34.
[2] Joyce JA, Fearon DT. T cell exclusion, immune privilege, and the tumor microenvironment. Science 2015 Apr;348(6230):74–80.
[3] Becker JC, Andersen MH, Schrama D, Straten PT. Immune-suppressive properties of the tumor microenvironment. CancerImmunol Immunother 2013 Jul;62(7):1137–48.
[4] Bianchi G, Borgonovo G, Pistoia V, Raffaghello L. Immunosuppressive cells and tumour microenvironment: Focus on mesenchymal stem cells and myeloid derived suppressor cells. Histol Histopathol 2011 Jul;26(7):941–51.
[5] Kalluri R, Zeisberg M. Fibroblasts in cancer. Nat Rev Cancer 2006 May;6(5):392–401.
[6] Elkhattouti A, Hassan M, Gomez CR. Stromal fibroblast in age-related cancer: role in tumorigenesis and potential as novel therapeutic target. Front Oncol 2015 Jul;27:5.
[7] Tang H, Qiao J, Fu YX. Immunotherapy and tumor microenvironment. Cancer Lett 2016 Jan 1;370(1):85–90.
[8] Amini MA, Abbasi AZ, Cai P, Lip H, Gordijo CR, Li J, et al. Combining tumor microenvironment modulating nanoparticles with doxorubicin to enhance chemotherapeutic efficacy and boost antitumor immunity. J Natl Cancer Inst 2018 Sep;14.
[9] Oestman A, Augsten M. Cancer-associated fibroblasts and tumor growth - bystanders turning into key players. Curr Opin Genet Dev 2009 Feb;19(1):67–73.
[10] Liao D, Luo Y, Markowitz D, Xiang R, Reisfeld RA. Cancer associated fibroblasts promote tumor growth and metastasis by modulating the tumor immune microenvironment in a 4T1 murine breast cancer model. PLoS One 2009 Nov 23;4(11):e7965.
[11] Franco OE, Shaw AK, Strand DW, Hayward SW. Cancer associated fibroblasts in cancer pathogenesis. Semin Cell Dev Biol 2010 Feb;21(1):33–9.
[12] Gabrilovich DI, Nagaraj S. Myeloid-derived suppressor cells as regulators of the immune system. Nat Rev Immunol 2009 Mar;9(3):162–74.
[13] Mellman I, Coukos G, Dranoff G. Cancer immunotherapy comes of age. Nature 2011 Dec 21;480(7378):480–9.
[14] Ouyang L, Chang W, Fang B, Qin J, Qu X, Cheng F. Estrogen-induced SDF-1alpha production promotes the progression of ER-negative breast cancer via the accumulation of MDSCs in the tumor microenvironment. Sci Rep 2016 Dec;20(6):39541.
[15] Williams SA, Harata-Lee Y, Comerford I, Anderson RL, Smyth MJ, McColl SR. Multiple functions of CXCL12 in a syngeneic model of breast cancer. Mol Cancer 2010 Sep;17(9):250.
[16] Yang X, Lin Y, Shi Y, Li B, Liu W, Yin W, et al. FAP Promotes Immunosuppression by Cancer-Associated Fibroblasts in the Tumor Microenvironment via STAT3-CCL2 Signaling. Cancer Res 2016 Jul 15;76(14):4124–35.
[17] Shiga K, Hara M, Nagasaki T, Sato T, Takahashi H, Takeyama H. Cancer-associated fibroblasts: their characteristics and their roles in tumor growth. Cancers 2015 Dec;7(4):2443–58.
[18] Orimo A, Weinberg RA. Stromal fibroblasts in cancer - A novel tumor-promoting cell type. Cell Cycle 2006 Aug 1;5(15):1597–601.
[19] Acharya PS, Zukas A, Chandan V, Katzenstein A-LA, Puré E. Fibroblast activation protein: a serine protease expressed at the remodeling interface in idiopathic pulmonary fibrosis. Hum Pathol 2006;37(3):352–60.
[20] Mentlein R, Hattermann K, Hemion C, Jungbluth AA, Held-Feindt J. Expression and role of the cell surface protease seprase/fibroblast activation protein-alpha (FAP-alpha) in astroglial tumors. Biol Chem 2011 Mar;392(3):199–207.
[21] Garin-Chesa P, Old LJ, Rettig WJ. Cell surface glycoprotein of reactive stromal fibroblasts as a potential antibody target in human epithelial cancers. Proc Nat Acad Sci USA 1990-Sep;87(18):7235–9.
[22] Pure E, Blomberg R. Pro-tumorigenic roles of fibroblast activation protein in cancer: back to the basics. Oncogene 2018 Aug;37(32):4343–57.
[23] Rettig WJ, Garin-Chesa P, Healey JH, Su SL, Ozer HL, Schwab M, et al. Regulation and heteromeric structure of the fibroblast activation protein in normal and transformed cells of mesenchymal and neuroectodermal origin. Cancer Res 1993-Jul-15;53(14):3327–35.
[24] Kraman M, Bambrough PJ, Arnold JN, Roberts EW, Magiera L, Jones JO, et al. Suppression of antitumor immunity by stromal cells expressing fibroblast activation protein-alpha. Science 2010 Nov 5;330(6005):827–30.
[25] Fassnacht M, Lee J, Milazzo C, Boczkowski D, Su Z, Nair S, et al. Induction of CD4(+) and CD8(+) T-cell responses to the human stroma antigen, fibroblast activation protein: Implication for cancer immunotherapy. Clin Cancer Res 2005 Aug 1;11(15):5566–71.
[26] Xia Q, Zhang FF, Geng F, Liu CL, Xu P, Lu ZZ, et al. Anti-tumor effects of DNA vaccine targeting human fibroblast activation protein alpha by producing specific immune responses and altering tumor microenvironment in the 4T1 murine breast cancer model. CancerImmunol Immunother 2016 May;65(5):613–24.
[27] Huang Y, Simms AE, Mazur A, Wang S, Leon NR, Jones B, et al. Fibroblast activation protein-alpha promotes tumor growth and invasion of breast cancer cells through non-enzymatic functions. Clin Exp Metastasis 2011 Aug;28(6):567–79.
[28] Wonganu B, Berger BW. A specific, transmembrane interface regulates fibroblast activation protein (FAP) homodimerization, trafficking and exopeptidase activity. Biochim Biophys Acta 2016 Aug;1858(8):1876–82.
[29] Delogu G. DNA vaccine combinations expressing either tissue plasminogen activator signal sequence fusion proteins or ubiquitin-conjugated antigens induce sustained protective immunity in a mouse model of pulmonary tuberculosis. Infect Immun 2002;70(1):292–302.
[30] Luo M, Tao P, Li J, Zhou S, Guo D, Pan Z. Immunization with plasmid DNA encoding influenza A virus nucleoprotein fused to a tissue plasminogen activator signal sequence elicits strong immune responses and protection against H5N1 challenge in mice. J Virol Methods 2008 Dec;154(1–2):121–7.
[31] Kou Y, Xu Y, Zhao Z, Liu J, Wu Y, You Q, et al. Tissue plasminogen activator (tPA) signal sequence enhances immunogenicity of MVA-based vaccine against tuberculosis. Immunol Lett 2017 Oct;190:51–7.
[32] Xia Q, Geng F, Zhang FF, Liu CL, Xu P, Lu ZZ, et al. Enhancement of fibroblast activation protein alpha-based vaccines and adenovirus boost immunity by cyclophosphamide through inhibiting IL-10 expression in 4T1 tumor bearing mice. Vaccine 2016 Aug 31;34(38):4526–35.
[33] Wang YQ, Zhang HH, Liu CL, Wu H, Wang P, Xia Q, et al. Enhancement of survivin-specific anti-tumor immunity by adenovirus prime protein-boost immunity strategy with DDA/MPL adjuvant in a murine melanoma model. Int Immunopharmacol 2013 Sep;17(1):9–17.
[34] Gottschalk S, Yu F, Ji M, Kakarla S, Song XT. A vaccine that co-targets tumor cells and cancer associated fibroblasts results in enhanced antitumor activity by inducing antigen spreading. PLoS One 2013;8(12):e82658.
[35] Loeffler M, Kruger JA, Niethammer AG, Reisfeld RA. Targeting tumor-associated fibroblasts improves cancer chemotherapy by increasing intratumoral drug uptake. J Clin Invest 2006 Jul;116(7):1955–62.
[36] Wen Y, Wang CT, Ma TT, Li ZY, Zhou LN, Mu B, et al. Immunotherapy targeting fibroblast activation protein inhibits tumor growth and increases survival in a murine colon cancer model. Cancer Sci 2010 Nov;101(11):2325–32.
[37] Ostrand-Rosenberg S, Fenselau C. Myeloid-derived suppressor cells: immune-suppressive cells that impair antitumor immunity and are sculpted by their environment. J Immunol 2018 Jan 15;200(2):422–31.

[38] Adachi K, Kano Y, Nagai T, Okuyama N, Sakoda Y. Tamada K. IL-7 and CCL19 expression in CAR-T cells improves immune cell infiltration and CAR-T cell survival in the tumor. Nat Biotechnol 2018 Apr;36(4):346-+.
[39] Bagley SJ, Desai AS, Linette GP, June CH, O'Rourke DM. CAR T-cell therapy for glioblastoma: recent clinical advances and future challenges. Neuro-oncology 2018-Oct-09;20(11):1429–38.
[40] Porter DL, Levine BL, Kalos M, Bagg A, June CH. Chimeric antigen receptor-modified T cells in chronic lymphoid leukemia. N Engl J Med 2011 Aug 25;365 (8):725–33.
[41] Topalian SL, Hodi FS, Brahmer JR, Gettinger SN, Smith DC, McDermott DF, et al. Safety, activity, and immune correlates of anti-PD-1 antibody in cancer. N Engl J Med 2012 Jun 28;366(26):2443–54.
[42] Chen M, Xiang R, Wen Y, Xu G, Wang C, Luo S, et al. A whole-cell tumor vaccine modified to express fibroblast activation protein induces antitumor immunity against both tumor cells and cancer-associated fibroblasts. Sci Rep 2015 Sep;23(5):14421.
[43] Henry LR, Lee H-O, Lee JS, Klein-Szanto A, Watts P, Ross EA, et al. Clinical implications of fibroblast activation protein in patients with colon cancer. Clin Cancer Res 2007 Mar 15;13(6):1736–41.
[44] Yuan D, Liu B, Liu K, Zhu G, Dai Z, Xie Y. Overexpression of fibroblast activation protein and its clinical implications in patients with osteosarcoma. J Surg Oncol 2013 Sep;108(3):157–62.
[45] Jung YY, Lee YK, Koo JS. Expression of cancer-associated fibroblast-related proteins in adipose stroma of breast cancer. Tumor Biol 2015 Nov;36 (11):8685–95.
[46] Obermajer N, Wong JL, Edwards RP, Odunsi K, Moysich K, Kalinski P. PGE(2)-driven induction and maintenance of cancer-associated myeloid-derived suppressor cells. Immunol Invest 2012;41(6–7):635–57.